

A Super-Nyquist Architecture for Reliable Underwater Acoustic Communication

Uri Erez
Tel Aviv University
Ramat Aviv, Israel
Email: uri@eng.tau.ac.il

Gregory Wornell
Dept. EECS, MIT
Cambridge, MA
Email: gww@mit.edu

Abstract—A natural joint physical and link layer transmission architecture is developed for communication over underwater acoustic channels, based on the concept of super-Nyquist (SNQ) signaling. In such systems, the signaling rate is chosen significantly higher than the Nyquist rate of the system. We show that such signaling can be used in conjunction with good “off-the-shelf” base codes, simple linear redundancy, and minimum mean-square error decision feedback equalization (MMSE-DFE) to produce highly efficient, low complexity rateless (i.e., “fountain”) codes for the severe time-varying intersymbol-interference channels typical of this application. We show that not only can SNQ rateless codes approach capacity arbitrarily closely, but even particularly simple SNQ-based rateless codes require the transmission of dramatically fewer packets than does traditional ARQ with Chase combining.

I. INTRODUCTION

The design of reliable, high-speed digital communication links for the underwater acoustic (UWA) channel is particularly challenging. Indeed, typically the medium is both highly dispersive and dynamic. Over the years, considerable progress has been made in meeting these challenges. A review of some of these advances can be found in, e.g., [1]–[3].

To meet the requirements of emerging applications, considerable further advances will be required. In particular, while traditional work in the area has largely focused on the physical layer, the key to future advances will be careful and joint design of the physical and link layers in underwater acoustic modems. Specifically, through such design one aim is for systems that dynamically adapt to the highly variable maximum instantaneous rate supported by the medium, and thereby achieve the highest possible throughput.

The typical approach to ensuring high throughput when the channel state allows is to exploit higher-order signal constellations. However, an alternative approach, originally proposed several decades ago [4], is to exploit super-Nyquist (SNQ) (equivalently referred to as faster-than-Nyquist) signaling. In SNQ signaling, the symbols are taken from a fixed constellation, typically BPSK or QPSK, independent of the transmission rate. Higher rates are achieved by increasing the signaling rate—i.e., the rate at which the symbols are modulated onto the bandlimited pulse shape—beyond the

Nyquist rate. Thus, in SNQ systems, the signaling rate is decoupled from the transmission bandwidth, and can greatly exceed the transmission bandwidth.

The relative merits of SNQ modulation with respect to the more standard Nyquist-rate modulation have been studied from different perspectives over the past four decades; see, e.g., [5]. The most significant drawback to using SNQ signaling is that it introduces severe intersymbol interference (ISI). For a channel with a flat frequency response, or having an ISI span of short duration, this is a major disadvantage. This is particularly so for a coded system, as it greatly increases the complexity of equalization and decoding. Largely for this reason, SNQ signaling was not widely adopted for many of the early applications of digital communication.

By contrast, even with Nyquist signaling, UWA channels suffer from severe ISI, and thus the additional ISI introduced by employing SNQ signaling is much less significant. In fact, for the most part, it can be well handled by the existing equalization implemented in such systems. As such, SNQ signaling is a feasible candidate for future underwater acoustic modems.

In this paper, we establish that not only is SNQ signaling feasible for the UWA channel, it has some particularly valuable properties for this and other related applications. In particular, we establish the somewhat surprising result that the use of SNQ signaling allows for highly efficient link layers designs. Indeed, from such signaling we develop a rich family of low-complexity, capacity-approaching rateless codes for ISI channels, which gracefully accommodate the highly dynamic nature of the UWA channel.

To develop this perspective, we begin by noting that in a typical packetized transmission scheme, data is partitioned into blocks that are sequentially sent over the channel. If the channel were time-invariant, the rate of a packet could be set arbitrarily close to the capacity of the channel. The UWA channel however exhibits fast variation and therefore the transmitter does not have accurate knowledge of the maximal rate it can support. Therefore, in the absence of feedback the transmitter must resort to setting the rate chosen for a packet based on an estimate or prediction of the instantaneous capacity of the channel. To achieve a low probability of packet loss (outage), one is generally forced to take a conservative approach and choose a sufficiently low rate, resulting in a

This work was supported in part by the ONR under MURI Grant No. N00014-07-1-0738, by AFOSR under Grant No. FA9550-11-1-0183, and by the Israel Science Foundation under Grant No. 1557/10.

throughput that is far from the capacity of the realized channel.

In many scenarios, however, a low rate feedback link is established between the two transmission ends, over which an acknowledgement (either positive or negative) can be sent back to the transmitter. When such a link is available, a much higher target rate for a given packet may be chosen.¹ When the receiver is unable to decode a packet, rather than treating the event as an outage, retransmission of some form is employed, the simplest example of which is repetition of the packet.

While repetition is a particularly simple means to attain greater redundancy, it is very inefficient. Numerous superior methods for achieving variable levels of redundancy via retransmissions have been proposed and studied; for instance, punctured codes are often used. Such error correction mechanisms are referred to as (hybrid) ARQ protocols, and the codes that support variable-rate transmission are referred to as incremental-redundancy (IR) codes. An IR code has the property that when truncated to a shorter length, it results in a good code of higher rate. Thus, a single IR code may support multiple rates by varying the length of the code transmitted.

In some scenarios an even stronger property is required—viz., the code must be good (i.e., with respect to the total “received blocklength”) when *any* subcollection of the transmitted packets are dropped. A code possessing this property is sometimes referred to as a fountain code [6]. In this paper, we refer to it as a variable-redundancy (VR) code.

As the main contribution of this paper, we develop a simple, yet highly efficient, VR coding scheme utilizing SNQ signaling. In the proposed scheme, a standard “off-the-shelf” fixed-rate based code, designed to achieve reliable transmission over a standard additive white Gaussian noise (AWGN) channel, is used in conjunction with linear processing and decision-feedback equalization, to obtain a VR transmission architecture.

The VR coding architecture developed in this paper is related to the family of IR redundancy codes developed for the AWGN channel in [7] [8] in that it is based on layering (superposition), dithering, and successive interference cancellation. Indeed, in one respect, this paper represents the extension of such methods to ISI channels. However, it also worth noting in advance that whereas the coding scheme of [7] is limited to IR coding, the present work develops a VR scheme. In this respect, the architecture developed in this paper is more closely related to that of [9], which derives a VR coding scheme for Gaussian MIMO channels. At the same time, the scheme developed in this paper may be viewed as a significant generalization of one in [10], which developed a SNQ VR-coding scheme for the AWGN channel. The scheme in [10] was somewhat both less efficient and less practical, owing to the use of random dithering rather than the more judiciously chosen (deterministic) modulation we exploit in this work.

¹It is important to emphasize that if there is significant delay in the feedback link, this affects the latency of the overall scheme, but need not affect the throughput by appropriate use of multiplexing.

II. SYSTEM AND CHANNEL MODEL

Consider a complex baseband representation of a linear dispersive Gaussian channel,

$$y(t) = h(t) * x(t) + z(t),$$

where $z(t)$ is AWGN noise with one-sided power spectral density N_0 . The input signal is subject to a power constraint $\mathbb{E}\{|x(t)|^2\} \leq P$.

We consider transmission over bandwidth W . For spectrally flat transmission over the band W , the resulting mutual information, which we refer to as the white-input capacity of the channel, is

$$C_{[b/s]} = \int_{-W/2}^{W/2} \log \left(1 + \frac{P|H(f)|^2}{N_0 W} \right) df. \quad (1)$$

A. Super-Nyquist Modulation

We assume pulse-amplitude modulation where the discrete-time input sequence is modulated to form a continuous-time input signal according to

$$x(t) = \sum_n s[n] \cdot g(t - n \cdot T), \quad (2)$$

where T is the symbol duration. We denote the Nyquist sampling time by $T^* = 1/W$. We further denote the “over-signaling” ratio by $L = T^*/T$.² We assume that at the receiver end, the signal is passed through a matched filter (MF), and sampling is performed at the symbol rate. This results in a discrete-time channel

$$y[n] = s[n] * k[n] + z[n], \quad (3)$$

where $k[n] = k(nT)$, where $k(t) = g(t) * g(-t)^* * h(-t) * h^*(-t)$, and where

$$\begin{aligned} S_{zz}(e^{j2\pi f}) &= \frac{N_0}{2} K(e^{j2\pi f}) \\ &= \frac{N_0}{2} \cdot \frac{1}{T} \sum_i |H(f/T + i/T)|^2 |G(f/T + i/T)|^2. \end{aligned}$$

The pulse shape is required to be limited to system bandwidth W , i.e., $g(t)$ satisfies

$$G(f) = 0 \quad \text{for } |f| > W/2. \quad (4)$$

To simplify our development, we initially restrict our attention to the ideal case where

$$g(t) = \text{sinc}(t/T^*), \quad \text{with } \text{sinc}(u) \triangleq \begin{cases} \frac{\sin(\pi u)}{\pi u} & u \neq 0, \\ 1 & u = 0. \end{cases} \quad (5)$$

We note that for an ideal (frequency flat) channel ($|H(f)| = 1$), the discrete-time channel response in this case becomes $k[n] = T^* \text{sinc}(n/L)$, so if we signal at the Nyquist rate, i.e., if $L = 1$, then $k[n] = T^* \delta[n]$ and no ISI is present. On the other hand, taking $L > 1$ necessarily introduces ISI.

²We assume that the over-signaling rate L is an integer for practical reasons.

Taking the symbols $s[n]$ to be i.i.d. circularly symmetric complex Gaussian with power P/L results in a (proper) Gaussian random input signal $x(t)$ with power P . It follows that the capacity of the discrete-time channel (3) is

$$\begin{aligned} C_{[\text{b/SNQ symbol}]} &= \int_{-1/2}^{1/2} \log \left(1 + \frac{(P/L) \cdot K(e^{j2\pi f})}{N_0} \right) df \\ &= T \int_{-1/2T}^{1/2T} \log \left(1 + \frac{P \sum_i |H(f+i/T)|^2 |G(f+i/T)|^2}{T^* N_0} \right) df \\ &= T \int_{-1/2T}^{1/2T} \log \left(1 + \frac{P/T^* |H(f)|^2 |G(f)|^2}{N_0} \right) df, \end{aligned} \quad (6)$$

where the last equality follows from (4).

Note that for sinc modulation, $x(t)$ has a flat power spectrum over the bandwidth W , yielding the mutual information given in (1), i.e., (6) reduces to

$$\begin{aligned} C_{[\text{b/SNQ symbol}]} &= \frac{T}{T^*} \frac{1}{W} C_{[\text{b/s}]} \\ &= \frac{1}{L} \frac{1}{W} \int_{-W/2}^{W/2} \log \left(1 + \frac{P|H(f)|^2}{N_0 W} \right) df. \end{aligned} \quad (7)$$

B. Linear SNQ Rateless Coding

Consider now packetized transmission where for notational convenience we let the time axis for the transmission of each packet be unbounded. We further consider a simplified model where the channel response experienced throughout transmission of the m th packet, $m = 1, \dots, M$, is linear time-invariant (LTI) but the impulse response, which we denote by $h_m(t)$, may vary from packet to packet. We assume for the moment that $M \leq L$. The channel input-output relation for the transmission of the m th packet is therefore

$$y_m[n] = s_m[n] * k_m[n] + z_m[n], \quad (8)$$

where $k_m[n] = k_m(l \cdot T)$ and $k_m(t) = g^*(-t) * g(t) * h_m^*(-t) * h_m(t)$. Assuming discrete-time white-input transmission for all packets, it follows from (7), that the mutual information (measured in b/SNQ symbol) corresponding to each packet is

$$\begin{aligned} C_m [\text{b/SNQ symbol}] &= \int_{-1/2}^{1/2} \log \left(1 + \frac{P K_m(e^{j2\pi f})}{N_0 L} \right) df \\ &= \frac{1}{L} \frac{1}{W} \int_{-W/2}^{W/2} \log \left(1 + \frac{P |H_m(f)|^2}{N_0 W} \right) df, \end{aligned}$$

where the second equality holds for ideal sinc modulation. Upon receiving a set $\mathcal{S} \subset \{1, \dots, M\}$ of packets, the aggregate mutual information is thus

$$C(\mathcal{S}) = \sum_{m \in \mathcal{S}} C_m. \quad (9)$$

Our aim is to design a low complexity coding and modulation scheme that (simultaneously) approaches $C(\mathcal{S})$ for all sets $\mathcal{S} \subset \{1, \dots, M\}$ without requiring the transmitter to have

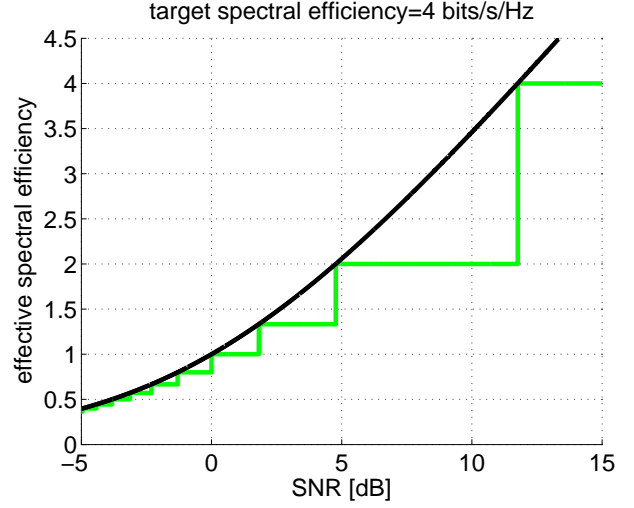


Fig. 1. Effective spectral efficiency as a function of SNR. The target spectral efficiency for transmission of a single packet is 4 b/s/Hz.

knowledge of the capacities C_m . Rather, for any given chosen target rate R , and no knowledge of the channel, transmission should be successful whenever $C(\mathcal{S}) > R$ holds for the received set of packets \mathcal{S} .

To illustrate the properties of such a scheme, Fig. 1 depicts the effective spectral efficiency as a function of the SNR, for the simple case of an ideal spectrally flat channel and sinc modulation. In this scenario we have

$$\begin{aligned} C(\mathcal{S})_{[\text{b/SNQ symbol}]} &= \frac{|\mathcal{S}|}{L} \log \left(1 + \frac{P}{N_0 W} \right) \\ &= |\mathcal{S}| C_1(\text{SNR}) \end{aligned}$$

where $\text{SNR} = P/(N_0 W)$. Thus, in an optimally designed (packetized) system, the number of required received packets as a function of the packet target rate R is given by

$$\text{number of packets required} = \lceil R/C_1(\text{SNR}) \rceil.$$

Accordingly, we define the effective spectral efficiency as the ratio of R to the number of required packets.

As a useful normalization, we further define the relative spectral efficiency as the fraction of capacity that is achieved

$$\eta(\text{SNR}) = \frac{R}{\text{no. req'd packets} \times C_1(\text{SNR})} = \frac{R/C_1(\text{SNR})}{\lceil R/C_1(\text{SNR}) \rceil}.$$

The relative spectral efficiency, for a target rate of 4 b/s/Hz is depicted in Fig. 2. Clearly, the relative spectral efficiency will tend to one as the target rate increases (and correspondingly, the number of retransmissions). Nevertheless, as will be discussed in Section IV, there are practical reasons for not setting the target rate much greater than the anticipated rate the channel can support.

We proceed to describe the proposed linear rateless SNQ construction. All the signals $s_m[n]$ are obtained from a single coded stream $s[n]$ as follows

$$s_m[n] = v_m[n] s[n], \quad (10)$$

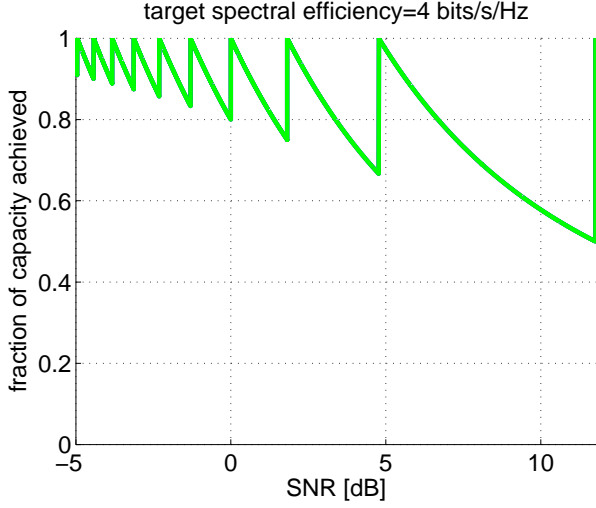


Fig. 2. Relative spectral efficiency as a function of SNR. The target spectral efficiency for transmission of a single packet is 4 b/s/Hz.

where $v_m[n]$ are sequences to be specified. The transmitted signal corresponding to packet m is thus

$$x_m(t) = \sum_i s[n] v_m[n] g(t - i \cdot T).$$

We now wish to choose the sequences $v_m[n]$ so that the transmitted signals $x_m(t)$ are statistically independent, and $s_m[n]$ are white circularly-symmetric complex Gaussian processes. This condition ensures that the mutual information corresponding to each packet remains C_m and furthermore than upon receiving multiple packets, the aggregate mutual information is the sum of the individual ones.

A simple means to achieve this is by taking each of the sequences $v_m[n]$ to be a discrete Fourier transform (DFT) sequence with frequencies being multiples of the oversampling rate $1/L$. Specifically, we take

$$v_m[n] = e^{-j2\pi mn/L}.$$

Let us now denote

$$x_m[n] = x_m(nT) = \sum_i s[i] e^{-j2\pi im/L} g^{\text{SNQ}}[n - i],$$

where $g^{\text{SNQ}}[n] = g(nT) = \text{sinc}(n/L)$, with $g(t)$ denoting a Nyquist-rate sinc pulse as specified in (5). Notice that each of the signals $s[n] e^{-j2\pi nm/L}$ is simply $s(\cdot)$ cyclicly shifted by m/L in the SNQ frequency domain. Let us denote the “shifted back” transmit signals by

$$\begin{aligned} x'_m[n] &= x_m[n] e^{j2\pi mn/L} \\ &= e^{j2\pi mn/L} \sum_i s[i] e^{-j2\pi im/L} g^{\text{SNQ}}[n - i] \\ &= \sum_i s[i] e^{j2\pi(n-i)m/L} g^{\text{SNQ}}[n - i] \\ &= \sum_i s[i] g_m^{\text{SNQ}}[n - i], \end{aligned}$$

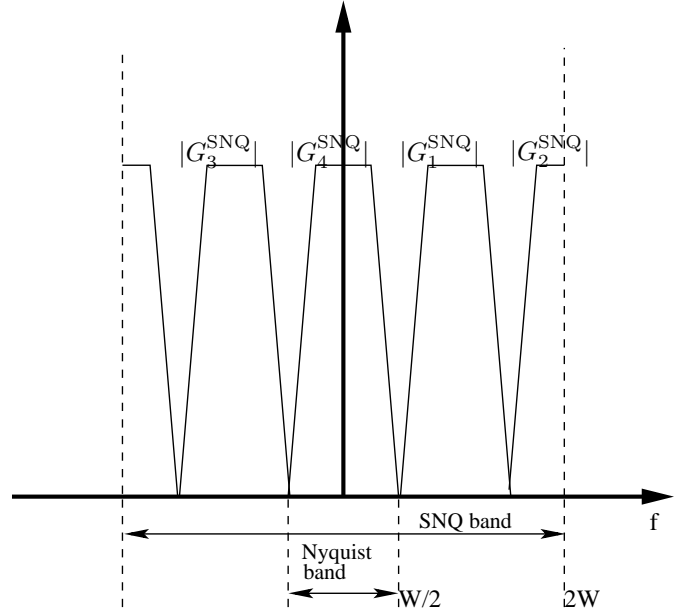


Fig. 3. Effective pulse shape for each packet occupies a different (non-overlapping) SNQ frequency band. Oversampling rate is $L = 4$.

where $g_m^{\text{SNQ}}[n] = e^{j2\pi mn/L} g^{\text{SNQ}}[n]$.

Observe that in $x'_m[n]$, rather than having the data sequence shifted in frequency, the modulation pulses $g_m^{\text{SNQ}}[n]$ are obtained by shifting $g^{\text{SNQ}}[n]$ in the SNQ frequency domain, as depicted in Fig. 3. This alternative view will be useful in the sequel.

Clearly, requiring that the signals $\{x_m(t)\}$ are mutually independent is equivalent to requiring that the associated discrete-time signals $\{x_m[n]\}$ are. Furthermore, the latter holds if and only if $\{x'_m[n]\}$ are mutually independent. Therefore, it suffices to verify the last condition. Since the signals $x'_m[n]$ are jointly Gaussian and stationary, they are independent if their cross spectra vanish. The latter are given by

$$\begin{aligned} S_{x'_{m_1} x'_{m_2}}(e^{j2\pi f}) &= S_{ss}(e^{j2\pi f}) G_{m_1}^{\text{SNQ}}(e^{j2\pi f}) G_{m_1}^{*\text{SNQ}}(e^{j2\pi f}) \\ &= \frac{1}{T^2} S_{ss}(e^{j2\pi f}) G\left(\frac{f + m_1/L}{T} \bmod \frac{1}{T}\right) \\ &\quad \cdot G^*\left(\frac{f + m_2/L}{T} \bmod \frac{1}{T}\right). \end{aligned}$$

Since $G(f/T)$ occupies no more than $1/L$ of the SNQ frequency band, it follows that there is no overlap between the frequency responses $G((f + m/L)/T \bmod 1/T)$ for different values of m , and hence $S_{x_{m_1} x_{m_2}}(e^{j2\pi f})$ indeed vanishes for $m_1 \neq m_2$; see Fig. 3.

In summary, the transmission architecture for our SNQ-based rateless code, depicted in Fig. 4 is as follows: the information bits are first encoded to form the code sequence $s[n]$, then the m th transmitted packet is generated by first

modulating $s[n]$ with a DFT sequence to obtain

$$s_m[n] = s[n]e^{-j2\pi mn/L},$$

The transmitted signal is then formed by modulating $s_m[n]$ according to (2).

III. MMSE-DFE EQUALIZATION

The modulation scheme developed is optimal in a mutual information sense. We now describe a low-complexity receiver architecture that suffices to approach the associated information-theoretic limits.

The front end of each receive element consists of matched filtering (i.e., ideal low-pass filtering for sinc modulation), followed by sampling at the SNQ rate WL . The discrete-time signals are given by (8). Taking into account the dithered transmission as given is (10), we have

$$y_m[n] = s[n]e^{-j2\pi mn/L} * k_m[n] + z_m[n].$$

We next “shift back” in frequency the received signal to obtain³

$$y'_m[n] = y_m[n]e^{j2\pi mn/L} = s[n] * k'_m[n] + z'_m[n],$$

where

$$K'_m(e^{j2\pi f}) = K_m(e^{j2\pi[f+m/L]}).$$

We have arrived at an equivalent single-input multiple-output LTI channel model, where $s[n]$ is the input signal and $y'_m[n]$ are the output signals. As the channels $K'_m(e^{j2\pi f})$ are non overlapping in frequency, they may be combined (summed) with no loss, resulting in an effective scalar ISI channel

$$\begin{aligned} y'[n] &= \sum_{m \in \mathcal{S}} y_m[n]e^{j2\pi mn/L} \\ &= s[n] * \left(\sum_{m \in \mathcal{S}} k'_m[n] \right) + \sum_{m \in \mathcal{S}} z'_m[n]. \end{aligned}$$

As the unbiased MMSE decision-feedback equalizer (DFE) results in a capacity-optimal receiver structure [11], [12] for such channels, we may apply it to our linear SNQ rateless coding scheme, as described next.

The DFE architecture for use in conjunction with our rateless construction is depicted in Fig. 5. The input to the slicer is formed as

$$\begin{aligned} \tilde{s}[n] &= a[n] * y'[n] - b[n] * \hat{s}[n] \\ &= \sum_{i=-\infty}^{\infty} a[i]y'[n-i] - \sum_{i=1}^{\infty} b[i]\hat{s}[n-i], \end{aligned} \quad (11)$$

where $a[n]$ are the feed-forward (FF) filters and $b[n]$ is a strictly causal feedback (FB) filter. The output of the slicer is denoted by $\hat{s}[n]$. Let $e[n] = s[n] - \tilde{s}[n]$ denote the “slicer error”, i.e., the effective noise at the slicer input. Assuming correct past decisions, then for optimal (unbiased) FF and FB

filters, invoking the optimality of the DFE receiver structure, we have that $e[n]$ is a stationary process satisfying

$$\log \left(1 + \frac{P/L}{\mathbb{E}[|e[n]|^2]} \right) = \sum_{m \in \mathcal{S}} C_m.$$

An alternative DFE structure is depicted in Fig. 6. Here, the output for each received packet is passed through a separate FF equalizer working at the Nyquist rate, so the input to the slicer is formed as

$$\tilde{s}[n] = \sum_{m \in \mathcal{S}} (a_m[n] * y'_m[n]) - b[n] * \hat{s}[n] \quad (12)$$

$$= \sum_{m \in \mathcal{S}} \sum_{i=-\infty}^{\infty} a_m[i]y'_m[n-i] - \sum_{i=1}^{\infty} b[i]\hat{s}[n-i]. \quad (13)$$

Note that the DFE loop must still work at the SNQ rate.

A. Extension: Multiple Hydrophones

The SNQ VR architecture can be applied to a system with multiple receive elements (hydrophones) essentially without change, as we briefly describe.

We denote the number of hydrophones by N_r , the channel from transmitter to receive element i by $h_m^i(t)$, and the associated discrete-time channel by $k_m^i[n]$. The equivalent received signal for packet m at receive element i is

$$y'^i_m[n] = s[n] * k'^i_m[n] + z'^i_m[n],$$

where

$$K'^i_m(e^{j2\pi f}) = K_m^i(e^{j2\pi[f+m/L]}).$$

Note that the frequency shift depends only on the packet, i.e., on m , but does not depend on the receive element i . The DFE receiver architecture remains essentially unchanged, now taking the form of multi-channel equalization, and is clearly still information lossless. The achievable rate is thus given by (9), where C_m (for sinc modulation) is now given by

$$\begin{aligned} C_m \text{ [b/SNQ symbol]} &= \frac{1}{L} \frac{1}{W} \int_{-W/2}^{W/2} \log \left(1 + \sum_{i=1}^{N_r} \frac{P|H_m^i(f)|^2}{N_0 W} \right) df. \end{aligned}$$

IV. PRACTICAL CONSIDERATIONS

In this section, we comment on at least some practical considerations that affect the deployed system. Among these are the implications of coding on the equalizer and error propagation effects; the impact of the choice of oversampling rate, and addressing the time-variation inherent in the channel.

A. Combining Decision-Feedback Equalization with Coding

While the unbiased MMSE DFE offers a capacity-optimal equalization architecture, it is well known that it is a rather difficult task to combine it with coding as is essential to approach capacity. In particular, the known approaches call for either using non-linear precoding (which necessitates channel knowledge at the transmitter), or very long Guess-Varanasi

³Note that the frequency shift operator is information lossless.

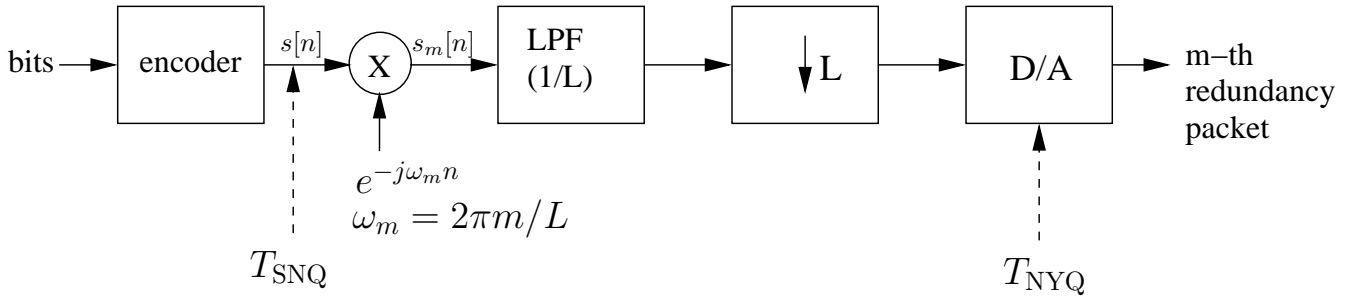


Fig. 4. Transmission of m th redundancy packet.

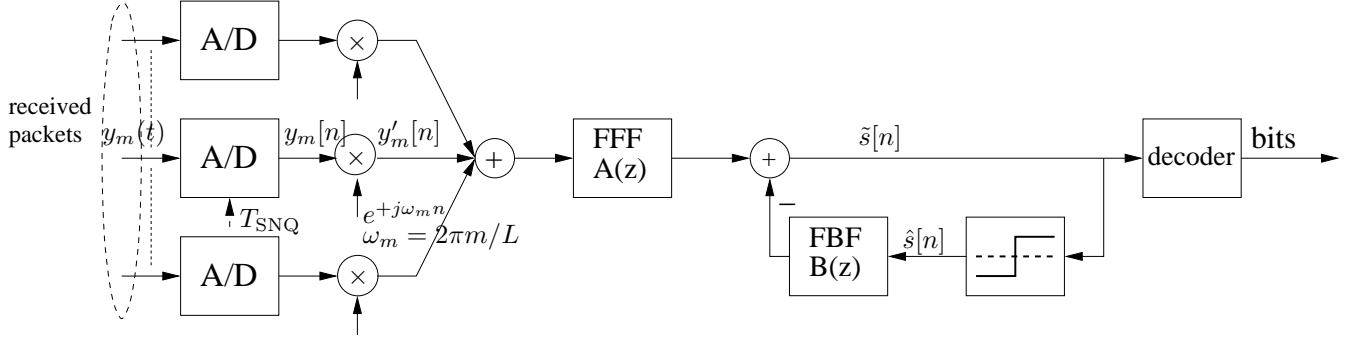


Fig. 5. Decision-feedback equalization architecture.

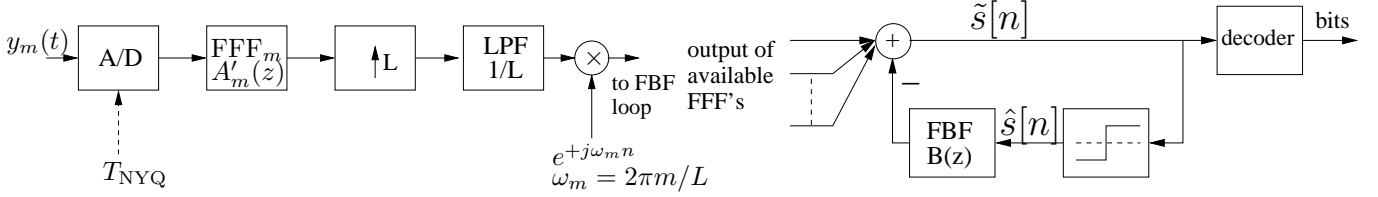


Fig. 6. Alternative decision-feedback equalization architecture using Nyquist-rate multichannel feedforward filters.

interleaving; see, e.g., [11], [12]. As neither approach is attractive for practical implementation, we opted to follow the well-established concatenated approach as depicted in Figs. 5 and 6, whereby the received signals are first processed as uncoded symbols. More specifically, with respect to equalization, the symbols $s[n]$ are treated as uncoded and decisions are made using a slicer. This results in an equalized signal $\tilde{s}[n]$ as described by (11) and (13). The latter signal is passed to a soft-input decoder to retrieve the information bits.

An inherent feature of SNQ signaling (in the case of SISO and SIMO transmission) is that the effective channel, as seen by the receiver, is strictly bandlimited as long as the number of received signals $|\mathcal{S}|$ is smaller than the SNQ rate L . This has a significant impact on the DFE operation as it results in severe error propagation. As a means to mitigate this adverse effect, delayed decision feedback may be used as described in [13]. It follows that there is a tradeoff between the dynamic range offered by the VR-SNQ scheme, which is captured by the SNQ rate L , and the complexity needed for adequate DFE equalization.

B. Hybrid DFT/Repetition Scheme

A pragmatic approach to counter the error propagation phenomenon described above, is to set the SNQ rate at a moderate level, say between 2 and 4, and when further redundancy packets are needed, allow for somewhat reduced performance. In the context of an ARQ protocol, where additional “redundancy packets” are sent sequentially, a simple means to achieve this goal, is to generate the first L dither sequences according to the columns of $L \times L$ DFT matrix, and then sequentially go through the same dither sequences for subsequent retransmissions. In other words, for $m > L$, we revert to repetition. Note that the special case of Nyquist signaling ($L = 1$) corresponds to traditional ARQ with Chase combining (ARQ-CC). As we will see, performance improves considerably relative to this baseline for $L > 1$.

For the case of an ideal channel, it is not difficult to show that the mutual information achieved by such a dithering scheme, when $m > L$ consecutive packets are received, is

given by

$$C_{\text{rep}}^{\text{DFT}}(\{1, \dots, m\})_{[\text{b/SNQ symbol}]}$$

$$= \frac{m^-}{L} \log \left(1 + \left\lfloor \frac{m}{L} \right\rfloor \text{SNR} \right)$$

$$+ \frac{m^+}{L} \log \left(1 + \left\lceil \frac{m}{L} \right\rceil \text{SNR} \right),$$

where $m^+ = m - \lfloor 1/L \rfloor L$ and $m^- = L - m^+$. On the other hand, a simple upper bound, based on dimensionality considerations, may be obtained for the maximal possible mutual information $C_{L\text{-SNQ}}(\{1, \dots, m\})$, attainable with any possible choice of sequences $v_1[n], \dots, v_m[n]$. Specifically, for $m > L$, $C_{L\text{-SNQ}}(\{1, \dots, m\})$ must satisfy

$$C_{L\text{-SNQ}}(\{1, \dots, m\})_{[\text{b/SNQ symbol}]}$$

$$\leq \log \left(1 + \frac{m}{L} \text{SNR} \right). \quad (14)$$

From (14) it is straightforward to obtain a bound on the spectral efficiency r of the hybrid DFT/repetition scheme as a function of SNR for a given target rate R and oversampling factor L . In particular, from the equality

$$r = \frac{R}{m} \leq \frac{L}{m} \log \left(1 + \frac{m}{L} \text{SNR} \right)$$

we obtain, with R and r in b/s/Hz,

$$r \leq \frac{R/L}{2^{R/L} - 1} \text{SNR}. \quad (15)$$

In turn, the spectral efficiency relative to a perfect scheme ($r = \log(1 + \text{SNR})$) is bounded by

$$\eta \leq \frac{R \ln(2)/L}{e^{(R \ln(2)/L)} - 1} \frac{\text{SNR}}{\ln(1 + \text{SNR})}$$

$$\rightarrow \frac{(R/L) \ln(2)}{2^{R/L} - 1} \quad \text{as } \text{SNR} \rightarrow 0. \quad (16)$$

Finally, by similar analysis, the spectral efficiency gain relative to Nyquist signaling (i.e., ARQ-CC) in the limit of low SNR is

$$\gamma = \frac{(2^R - 1)/L}{2^{R/L} - 1}. \quad (17)$$

Fig. 7 depicts the effective spectral efficiency attained η using the hybrid DFT/repetition scheme along with the upper bound (14), as well as the performance of DFT dithering with $L \rightarrow \infty$ (as was depicted above in Fig. 1).

Fig. 8 depicts the corresponding relative efficiency η achieved. From (16), we see that the upper and lower curves in the figure converge to relative spectral efficiencies of $\eta = 0.462$ and $\eta = 0.185$, respectively, in the limit of low SNR. The lower curve reflects the well-known striking inefficiency of ARQ-CC: in this limit it requires sending more than 5.4 times the number of packets as a capacity achieving scheme such as SNQ with $L \rightarrow \infty$.

The ratio of the two curves in Fig. 8 yields the spectral efficiency gain γ of hybrid SNQ DFT/repetition with $L = 2$ relative to Nyquist signaling and repetition coding (ARQ-CC). From (17), we obtain that $\gamma \rightarrow 5/2$ as $\text{SNR} \rightarrow 0$, which translates to requiring the transmission of 60% fewer packets, even for this simplest implementation of SNQ signaling.

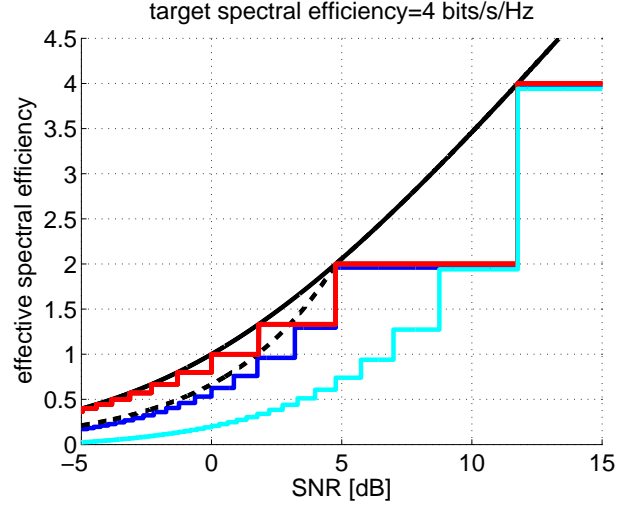


Fig. 7. Effective spectral efficiency as a function of SNR for rateless SNQ signaling, and for Nyquist signaling with repetition ($L = 1$). The target spectral efficiency for transmission of a single packet is 4 b/s/Hz. Curves from top to bottom: optimal, SNQ with DFT dithering with $L \rightarrow \infty$, hybrid SNQ ($L = 2$) DFT/repetition, and Nyquist signaling ($L = 1$) with repetition coding (ARQ-CC). Dashed line is the bound (15).

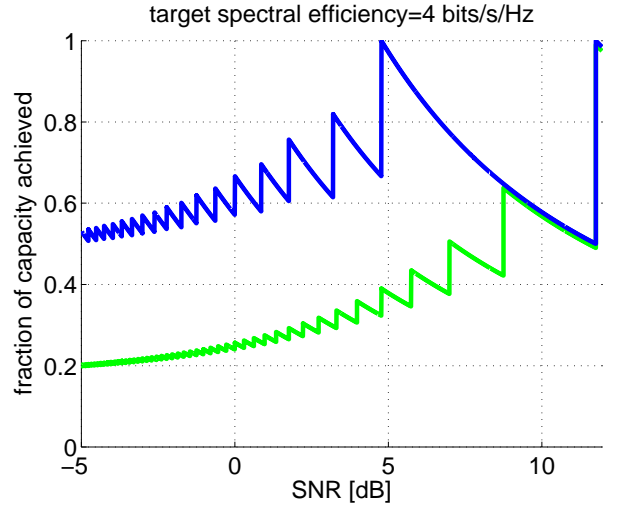


Fig. 8. Relative spectral efficiency as a function of SNR for hybrid SNQ DFT/repetition signaling with $L = 2$ and for Nyquist signaling ($L = 1$) where repetition is used for $m > L$. The target spectral efficiency for transmission is 4 b/s/Hz.

C. Adaptive Filtering

In principle, any adaption algorithm approach may be used to adapt the FF and FB filters at the receiver. Nevertheless, as the UWA channel is characterized by fast variation, performance will greatly be affected by the choice of algorithm and the associated complexity invested. In the experiment carried out, recursive least squares (RLS) adaptation was employed.

V. EXPERIMENTAL RESULTS

In this section, we demonstrate some preliminary performance plots based on data from the recent KAM11 experiment

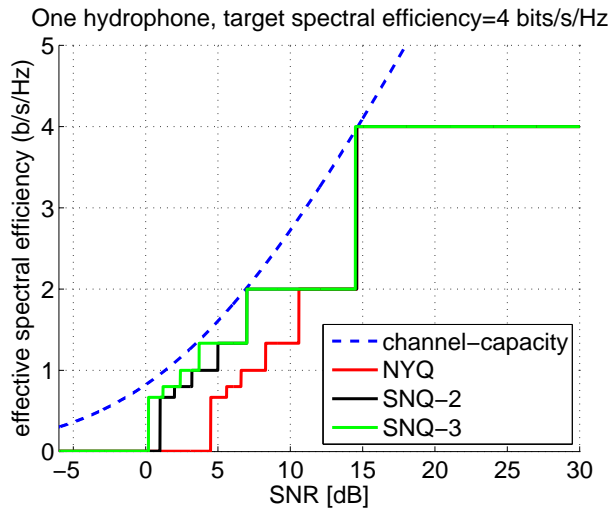


Fig. 9. Effective spectral efficiency as a function of SNR for rateless SNQ signaling, and for Nyquist signaling with repetition ($L = 1$), with ideal coding, on a snapshot of a KAM11 UWA channel snapshot.

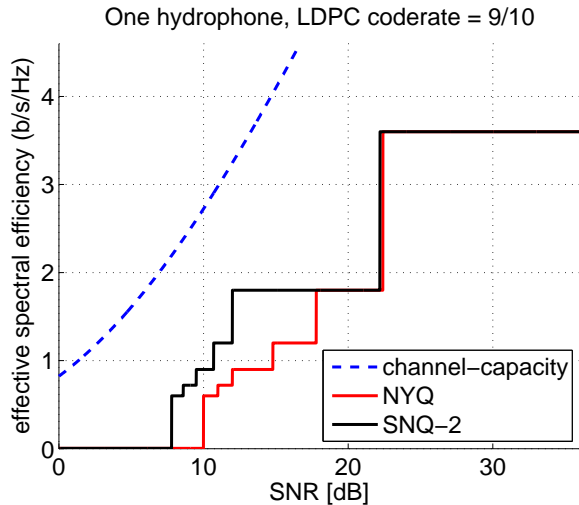


Fig. 10. Effective spectral efficiency as a function of SNR for QPSK rateless SNQ signaling, and for 16-QAM Nyquist signaling with repetition ($L = 1$), with a practical rate 9/10 LDPC code, on a snapshot of a KAM11 UWA channel snapshot.

off the coast of Hawaii.

First, in Fig. 9 we show for a sample snapshot of the channel during the experiment, the ultimate spectral efficiencies achievable by the different signaling strategies (with ideal coding). In Fig. 10, we show the corresponding results when a practical rate 9/10 code is used (and the code is ignored in feeding back decisions).

Finally, in Fig. 11 we plot the ultimate spectral efficiencies achievable from directly processing the data from a sample transmission in the KAM11 experiment (with ideal coding). Since the different signaling methods were used at slightly different times, and since the channel was changing rapidly, detailed direct comparisons are difficult, but the trends are

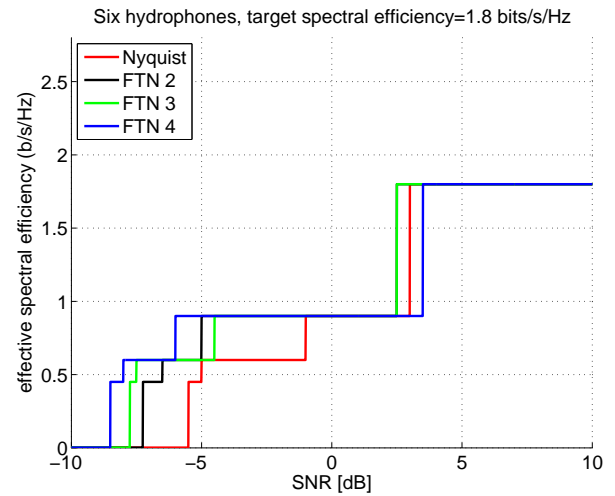


Fig. 11. Effective spectral efficiency as a function of SNR for rateless SNQ signaling, and for Nyquist signaling with repetition ($L = 1$), with ideal coding, from directly processing KAM11 data.

reflective of the performance potential.

ACKNOWLEDGMENT

The authors thank Qing He for her contributions to the simulations and experimental results included in the paper.

REFERENCES

- [1] M. Stojanovic, "Recent advances in high-speed underwater acoustic communications," *IEEE J. Ocean. Eng.*, vol. 21, pp. 125–136, Apr. 1996.
- [2] M. Stojanovic, "Underwater acoustic communications: Design considerations on the physical layer," in *Proc. Conf. Wireless on-Demand Network Systems and Services (WONS)*, pp. 1–10, Jan. 2008.
- [3] M. Chitre, S. Shahabudeen, and M. Stojanovic, "Underwater acoustic communications and networking: Recent advances and future challenges," *Marine Techn. Soc. J.*, vol. 42, pp. 103–116, 2008.
- [4] J. E. Mazo, "Faster-than-Nyquist signaling," *Bell Sys. Techn. J.*, vol. 54, pp. 1451–1462, Oct. 1975.
- [5] G. J. Foschini, "Contrasting performance of faster binary signaling with QAM," *Bell Sys. Techn. J.*, vol. 63, pp. 1419–1445, Oct. 1984.
- [6] M. Luby, "LT codes," in *Proc. IEEE Symp. Found. Comp. Sc. (FOCS)*, 2002.
- [7] U. Erez, M. D. Trott, and G. W. Wornell, "Rateless coding and perfect rate-compatible codes for Gaussian channels," in *Proc. IEEE Int. Symp. Inform. Theory (ISIT)*, (Seattle, WA), pp. 528–532, July 2006.
- [8] U. Erez, M. D. Trott, and G. W. Wornell, "Rateless coding for Gaussian channels," *IEEE Trans. Inform. Theory*, 2012. To appear.
- [9] M. M. Shaneshi, U. Erez, K. P. Boyle, and G. W. Wornell, "Time-invariant rateless codes for MIMO channels," in *Proc. IEEE Int. Symp. Inform. Theory (ISIT)*, pp. 2247–2251, July 2008.
- [10] U. Erez, G. W. Wornell, and M. D. Trott, "Coding for Faster-than-Nyquist signaling: The merits of a regime change," in *Proc. Allerton Conf. Commun., Contr., Computing*, (Monticello, IL), Sep. 2004.
- [11] T. Guess and M. K. Varanasi, "An information-theoretic framework for deriving canonical decision-feedback receivers in Gaussian channels," *IEEE Trans. Inform. Theory*, vol. 51, pp. 173–187, Jan. 2005.
- [12] G. D. Forney, Jr., "Shannon meets Wiener II: On MMSE estimation in successive decoding schemes," in *Proc. Allerton Conf. Commun., Contr., Computing*, (Monticello, IL), Oct. 2004.
- [13] A. Duel-Hallen and C. Heegard, "Delayed decision-feedback sequence estimation," *IEEE Trans. Commun.*, vol. 37, pp. 428–436, May 1989.